CFD Simulation of Flow−Induced Floating−Body Motions

Y. Xing, I. Hadzic, S. Muzaferija [a] and M. Peric

Fluid Dynamics and Ship Theory Section, Technical University of Hamburg−Harburg,
Laemmersieth 90, 22305 Hamburg, Germany

[a] ICCM, Bramfelder Strasse 164, 22305 Hamburg, Germany

Abstract

The techniques of Computational Fluid Dynamics (CFD) are applied to simulate floating−body motions in free−surface flow (e.g. waves). It is demonstrated that a wide variety of problems associated with the coupled analysis of flow and flow−induced body motions can be dealt with by a single computer code, which solves the Navier−Stokes equations and the equations of motion for a floating body in a coupled manner. The method is relevant to a wide range of applications in ship and ocean engineering, such as ship seakeeping and maneuvering etc. In this paper, a series of predictions of floating−body motions in waves and in other flows is discussed and comparisons between calculations and measurements are also presented.

I Introduction

Ship motions and associated loads on a ship hull can only be predicted fairly accurately using methods based on potential flow assumptions. Large errors can be introduced by these assumptions for a few practically important cases like ships' motions in large amplitude waves, ships' responses under a wave impact load (slamming), or ship capsizing etc. The need for a numerical tool that can predict the motions and loads in large waves, taking into account viscous effects, turbulence, flow separation and wave−breaking phenomena is obvious.

The objective of this research is to develop and validate a computational technique for the coupled analysis of viscous flow and flow−induced body movements in large/irregular waves. In the present study, a finite volume method has been used, which can accommodate any type of grid, and is therefore applicable to complex geometry problems. SIMPLE algorithm [1] has been taken to couple the pressure field properly to the velocity field. HRIC (High−Resolution Interface Capturing) scheme [2] has been used to simulate the free surface and to achieve the sharpness of the interface between water and air.

For predicting the body movements, floating−body dynamics has been implemented into the program "Comet" [3] via user−coding; a fully−implicit predictor−corrector procedure has been employed, taking advantage of the iterative nature of the fluid−flow solver. By the use of moving grid strategies, the motions of the bodies are presented by the displaced and adapted grid system fitted to the bodies' surfaces. The body movements are calculated according to the forces obtained by integrating pressure and shear stress over body surface.

II Computation Procedure

1. Numerical Tank

Our numerical tank consists of a fluid domain with two phases (water and air) bounded by a layer of air on top, a bottom surface in water and four vertical boundaries. All boundaries can be physical ones if the fluid is really bounded, but otherwise they are imaginary ones. At one vertical boundary, the movement of a flapping wave−maker can be simulated by moving grid, or waves can be generated by giving inlet velocity at the corresponding section. Numerical beaches are incorporated near other imaginary boundaries so that no waves are reflected. At solid walls, no−slip conditions are applied.

Regular waves are generated by imposing appropriate inlet velocities at the wave−maker boundary. For testing the performance of the present numerical tank, the small amplitude waves with amplitude A = 0.001m, radian frequency ω = 17.73 (1/s) have been generated first. The numerical tank was set 10 wave−lengths long plus a double−sized damping zone. The results are presented below, as well as the comparisons with the analytical results according to potential theory [4].

Figure 1 shows the instantaneous displacement of the free surface at t = 8.0 s, the implicit three−time−

level scheme has been used for time integration. The sinusoidal wave profile is compared with the analytical solution in Fig. 2 at t = 6.0 s.

Furthermore, Fig. 3 compares the vertical distribution of the horizontal velocity amplitude and that of the vertical velocity amplitude at about 1.5 m away from the wave−maker obtained by the present calculation with the corresponding values given by the linear water−wave theory [4]. The agreements are very good.

Figure 4 shows an example wave profile of large amplitude, generated in the present numerical tank by prescribing a large inlet velocity. As it can be observed, the wave profile is unsymmetric about y = 0, the crests are steeper and the troughs flatter, as a result of the nonlinear effects. For comparison, the nonlinear 2^{nd}−order Stokes waves [4] are plotted together with the computed surface elevation. The agreement is not as good as for small−amplitude waves as the viscous effects become more important.

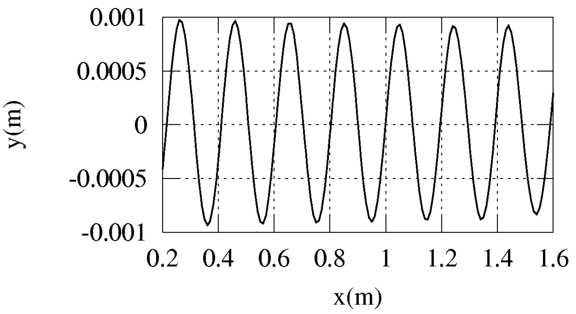

Fig. 1. Free surface profile at t = 8.0 s

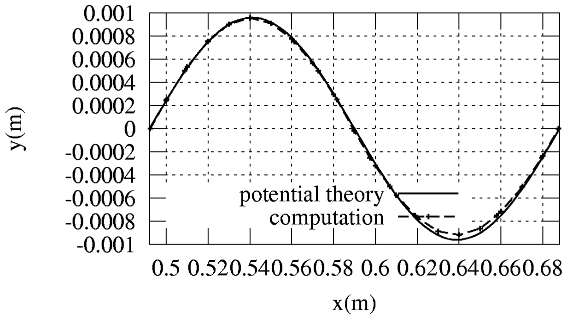

Fig. 2. Wave profile within one wave length

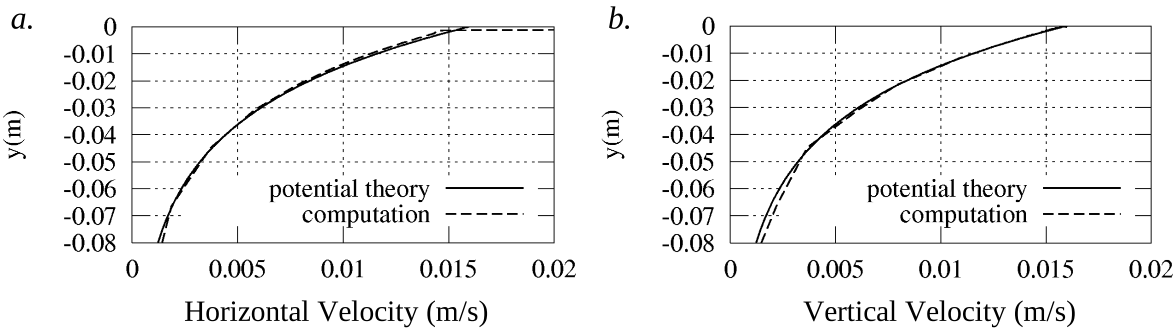

Fig. 3. The vertical distribution of velocity components at x = 1.5 m

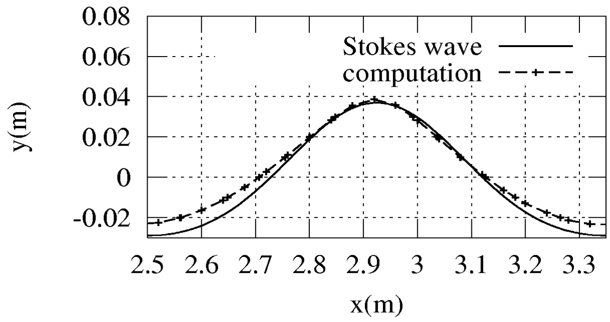

Fig. 4. Comparison of wave profiles, obtained in calculation and from the 2^{nd}−order Stokes theory

2. Floating bodies

For testing the reliability of the method for predicting the flow−induced body motions, a number of simple 2D−cases, with translation or rotation only, was analyzed first to verify the procedure and estimate the accuracy. Figure 5 shows one example of the test cases. The center of square cylinder is initially located at a distance of 1.25 D (D is cylinder width) below the free surface and is at rest as well as the fluid itself. The cylinder is free to move only in the vertical direction as it should be. After being released, due to the buoyancy force (density of the body is half of the water density), the cylinder first moves upwards and oscillates towards its equilibrium position. Figure 5.a shows the free−surface and the body position at time t = 0.6 s and Fig. 5.b shows the integral vertical force Fy, velocity Vc and position Yc of the body center as a function of time.

The horizontal lines in Fig. 5.b indicate the equilibrium states. Until at about 2 seconds, the strong damping of body movement due to viscous forces and generation of waves is present and then large oscillations of body are caused by the reflected waves from the vertical side walls of the channel (where no numerical beach is employed for this test case). A very complex situation is generated while the body breaks the free surface moving upwards and downwards with rapid change of force *Fy*, as shown in Fig. 5.b, representing the impingement of water at the body.

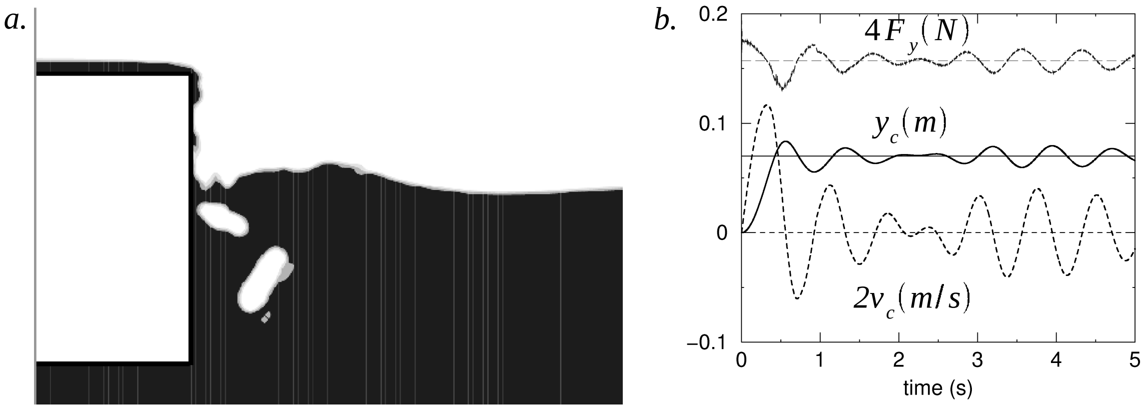

Fig. 5.a. The free−surface and the body position at time t = 0.6 s; b. The integral vertical force Fy, velocity Vc and position Yc of the body center as a function of time

3. Comparisons with experimental results

Since it has been confirmed that the basic performance of the present numerical tank is adequate for practical calculations associated with the wave−induced body motions, a series of computations is carried out, for which experiments can be executed for comparing the results.

a. Axis−fixed cylinder in waves

An experiment was set up for studying the axis−fixed cylinder motions in waves. The model has the dimensions of 12 cm width, 8 cm height and 20 cm length with the density of 665 kg/m^3, initially 3 cm submerged under the still water surface. The fixed−axis is set at 5.5 cm above the bottom edge of the cross section of the model. Waves are generated by simulating the flapping movements of the wave−maker in our towing tank. The wave−maker moves sinusoidally with the period of movement 0.7 s. Water depth of towing tank is 1.0 m. The waves have been reproduced and tested in our present numerical tank. Figure 6.a shows the free surface deformation and the body position at *t* = 6.82 s. Slamming occurs in such a situation: waves are broken in the vicinity of the body and an amount of water has been splashed on the top of body, as it can also be observed from the experiment. Figure 6.b shows the angular movements obtained from 2D calculation compared with experimental results. Since the 3D effect is significant in the experiment, the difference in the amplitude of the angular movement is reasonable. For further steps, 3D calculations are about to be set up by the authors.

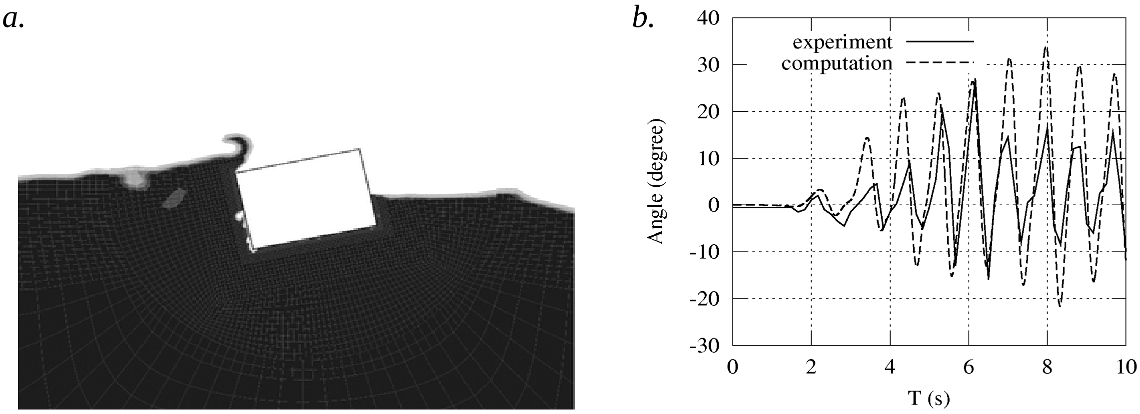

Fig. 6.a. The free surface deformation and the body position at t = 6.82 s; b. Comparison of the angular motion in experiment and calculation

b. Free−floating body in waves

The experiment of free−floating cylinder in waves was also set up in our towing tank. The body is made with 10 cm width, 5 cm height and 29 cm length, and with the density of 680 kg/m ^{3} . Both waves and body motions are compared with the experiment, as shown in Fig. 7. The agreement is rather good except at the initial stage, where the noise in the experiment is rather large. The fluid velocity vector profile at *t* = 4 s as well as the grid in the vicinity of the body are shown in Fig. 8, which gives some insight into the flow around the body and flow−body interaction.

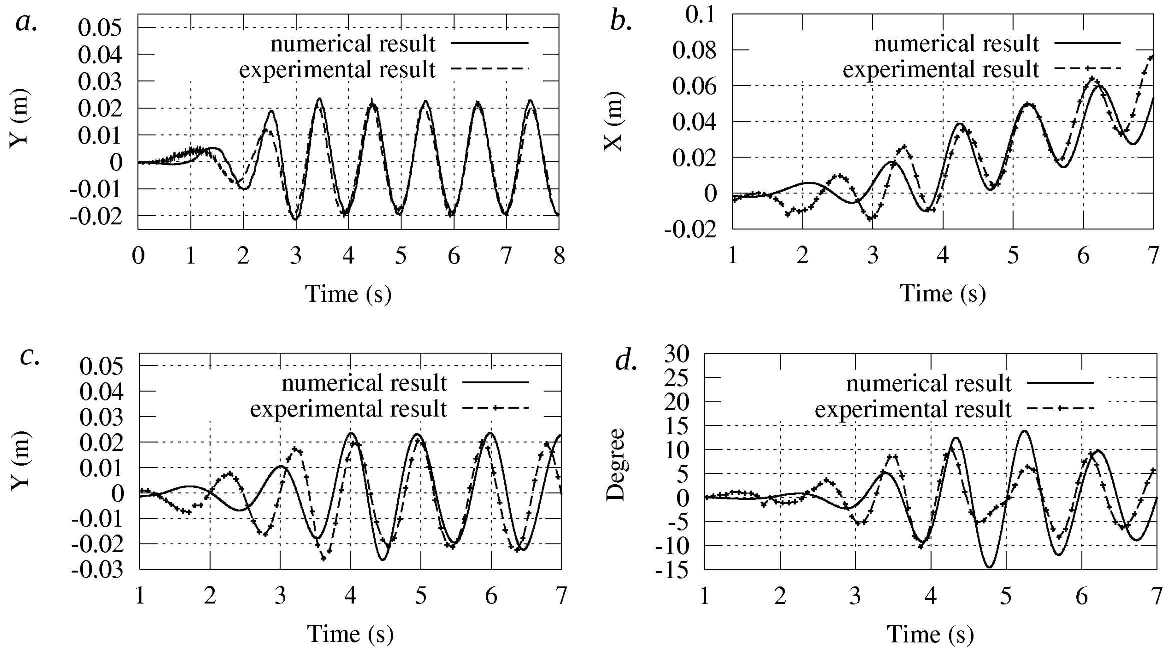

Fig. 7 a. The wave surface elevation at x = 1.5 m as a function of time; b., c., d. Comparison of free−floating body movements as a function of time in our computation and in the experimental results.

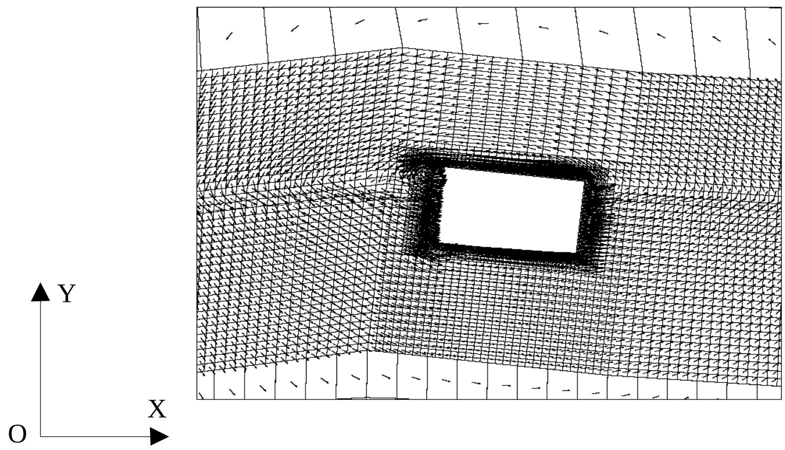

Fig. 8. The locally refined grid, fluid velocity vectors, and the body position at t = 4 s

References:

1. S. V. Patankar and D. B. Spalding: A calculation procedure for heat, mass and momentum transfer in three−dimensional parabolic flows, Int. J. Heat and Mass Transfer, 15:1787−1806, 1972.
2. S. Muzaferija and M. Peric: Computation of free−surface flows using interface−tracking and interface−capturing methods, chap. 2 in O. Mahrenholtz and M. Markiewicz (eds.), Nonlinear Water Wave Interaction, pp. 59−100, WIT Press, Southampton, 1999.
3. Comet user manual, ICCM (Institute of Computational Continuum Mechanics GmbH), Hamburg, 2000.
4. J. N. Newman: Marine Hydrodynamics, MIT Press, England, 1978.